TALLINN UNIVERSITY OF TECHNOLOGY
Faculty of Information Technology

IEE70LT

Yigit Aydog 146099IVEM

HUMAN MOVEMENT ESTIMATION BASED ON INERTIAL AND MULTILATERATION MEASUREMENTS

Master's Thesis

Supervisor: Alar Kuusik

PhD

Senior researcher

Tallinn 2016

TALLINNA TEHNIKAÜLIKOOL

Infotehnoloogia teaduskond

IEE70LT

Yigit Aydog 146099IVEM

INIMESE LIIKUMISE HINDAMINE INERTSIAALSETE JA MULTILATERATSIOONI MÕÕTMISTE BAASIL

Magistritöö

Juhendaja: Alar Kuusik

Dr.

Vanemteadur

Tallinn 2016

Author's declaration of originality

I hereby certify that I am the sole author of this thesis. All the used materials, references to the literature and the work of others have been referred to. This thesis has not been presented for examination anywhere else.

Author: Yigit Aydog

Date: 19.05.2016

Abstract

In this thesis, motivation for human motion tracking, detailed analysis of current motion tracking technologies that can be alternative to 'gold standard' optical motion tracking and integration possibilities of different motion tracking technologies are presented. In the first chapter, motivation for human motion velocity measurements, opportunities provided by wearable technology and alternatives to optical motion tracking are explained. First chapter concludes with introduction of project work and thesis motivation as a part of the project. The second chapter briefly explains the way of interpretation of human movement data and gives detailed analysis of inertial motion tracking systems. In the third chapter, emerging Ultra Wide Band radio indoor positioning technology and high precision GNSS systems are presented. Available Ultra Wide Band radio products from market and Ublox Neo-7P receiver are investigated in terms of their roles in movement tracking. Third chapter also includes author's contribution in the project. This thesis concludes with summary of all experiments, observations, comments of author and future work.

This thesis is written in English and is 51 pages long, including 4 chapters, 25 figures and 11 tables.

Annotatsioon

Käesolevas töö kirjeldatakse vajadusi, valitud tehnoloogilisi lahendusi ja nende integratsiooni inimese liikumise jälgimiseks, mis on alternatiiviks optilisele „kuldse standardile". Töö esimeses peatükis kirjeldatakse motivatsiooni inimese liikumiskiiruse hindamiseks, võimalusi, mida pakuvad kehal kantavad sensorid alternatiivina optilistele liikumise jälgimise meetoditele. Sissejuhatav peatükk lõpeb lõputöö motivatsiooni esitamisega. Teine peatükk kirjeldab lühidalt inimese liikumise interpreteerimist ja detailselt inertsiaalseid liikumise jälgimise süsteeme. Kolmandas peatükis esitletakse uudseid ultra-lairiba raadiol (UWB) ja täpsel satelliitlokatsioonil põhinevaid positsioneerimislahendusi. Käsitletakse konkreetseid UWB seadmeid ja Ublox Neo-7P vastuvõtjat. Kolmas peatükk sisaldab ka autori isikliku töö tulemusi. Töö lõpeb teostatud eksperimentide kokkuvõttega, jälgimise tulemustega, autori kommentaride ja edaspidise töö kirjeldusega.

Lõputöö on kirjutatud inglise keeles ning sisaldab teksti 51 leheküljel, 4 peatükki, 25 joonist, 11 tabelit.

List of abbreviations and terms

MEMS	Microelectromechanical systems
IMU	Inertial Measurement Unit
BSN	Body Sensor Networks
PDA	Personal Digital Assistant
QoS	Quality of Service
GNSS	Global Navigation Satellite System
UWB	Ultrawide band
PDR	Pedestrian Dead Reckoning System
PPM	Part Per Million
PSD	Power Spectral Density
PDF	Probability Distribution Function
DCM	Direct Cosine Matrix
MTw	Wireless Motion Tracker
LiPo	Lithium-ion Polymer Battery
SDK	Software Development Kit
ISM	Industrial Scientific Medical
ADC	Analog to Digital Converter
SDI	Strap Down Integration
ASCII	American Standard Code for Information Interchange
FCC	Federal Communications Commission
ECC	European Communications Committee
WPAN	Wireless personal area networks
WLAN	Wireless local area network
GSM	Global System for Mobile Communications
IR	Impulse Radio
PR	Pseudo random
RSSSI	Received signal strength indication
TH	Time hopping
PPM	Pulse Position Modulation

PAM	Pulse Amplitude Modulation
OOK	On off keying
SRD	Step Recovery Diode
LNA	Low Noise Amplifier
TOA	Time of Arrival
TDOA	Time Difference of Arrival
TOF	Time of flight
MS	Mobile Station
BS	Base Station
LOS	Line of Sight
NLOS	Non Line of Sight
INS	Inertial Navigation System
MEO	Medium Earth Orbit
GEO	Geostationary Orbit
SBAS	Satellite Based Augmentation Systems
DGPS	Differential GPS
GBAS	Ground Based Augmentation Systems
GPS	Global Positioning System
WAAS	Wide Area Augmentation System
EGNOS	The European Geostationary Navigation Overlay Service
ESA	European Space Agency
SDCM	System for Differential Corrections and Monitoring
GAGAN	Indian GPS Aided GEO Augmented Navigation
RTLS	Real Time Location System

Table of contents

1. INTRODUCTION

Motion tracking technologies are widely used to analyze human body movements in kinesiology, clinical, ambulatory studies and for athlete's performance evaluation in sport. The motion data is important for sport studies because every body movement such as running stride, pedal stroke and swim stroke represents unique movement pattern. The pattern analysis can pinpoint the body segments with loss of efficiency. Levels of mobility as physical activity frequency and motion intensity, stability, flexibility, and functional strength of athlete can be tracked from his/her body movement data so that sport coaches can interpret running patterns of athletes to enhance performance. Moreover, from early 1970s, experts in shoe manufacturing investigated how humans run and shock effect between the feet and ground to develop shoes with proper design and material. Therefore, movement of foot data can be used for designing running shoes. In medical studies, tracking body movements of patient gives chance for medical professionals to reveal biomechanical abnormalities in walking [1]. By knowing prior problems of biomechanics of patients, possible injuries can be predicted earlier. Overpronation and underpronation (supination) are some example of abnormalities which can be detected by observing motion of patient closely. After knowing impairments, medical professionals can subscribe exercise or rehabilitation program for each person according to abnormality of his/her motion. Finally, applications where motion data recording is required can be extended to separate tracking of parts of a whole moving system.

Kinematic analyses is generally conducted in laboratories equipped with optical motion tracking systems where cameras track the motion of patients or athletes. In marker based optical motion systems, the reflective markers are placed on subject's body segments and reflections are detected by cameras. By recording 2D position of markers in image coordinates during motion of subject and analyzing recorded data from all cameras with proprietary software, 3D position of subject at different time instants is determined. Highly sophisticated commercial motion tracking systems such as Vicon which uses reflective passive markers, coated with a retro-reflective material that reflects the light back to the cameras, or Optotrak which uses active markers, powered by small battery and emits their own light to cameras, are often considered as a 'gold standard' in human

motion analysis [2]. Over the years, they have become essential instrumentation in laboratories and specialized clinics and they can provide mm level accuracies [3].

Although optical motion tracking systems can track accurate 3D motion of a subject, they are not suited for portable data collection in the field where athletes have trainings [4]. Secondly, they are quite expensive devices with limited calibration volume and they often require post processing time. Therefore, there is a demand for small and unobtrusive devices which are capable of recording motion data regularly with high precision and provide it continuously in an easy way to interpret.

Wearable motion trackers usually include accelerometers, gyroscopes, GNSS receivers, digital compasses, inertial modules and pressure sensors enclosed in small and unobtrusive packages and have ability for wireless transmission of recorded data to hosting system for further processing and evaluation [5]. CCS Insight Ltd. (Slough, England) pointed out that shipments of wearable electronic devices grew from 9.7 million units in 2013 to 22 million units in 2014, an annual increase of 129 percent. Sales of wearable technology products come from smart watches, wristbands, wearable cameras, eyewear, tokens, clips-ons and jewelry. Many new applications have unfolded recently thanks to small, wireless and powerful inertial monitors. The examples of applications wearable electronics for wellbeing, sport and patients monitoring are given in [5] [6]

- Assisted living and monitoring of patients with function disorders using micromechanical (MEMS) sensors. Patients can be monitored for long time at home and outdoors.
- Monitoring patients with Parkinson's disease to improve clinical management of symptoms.
- Wearable fall detection units based on MEMS accelerometers.
- Activity, health and wellness monitoring.
- Biomechanics, athletic training optimization and other applications that require accurate orientation and kinematics of body segments.

With recent advances in low cost MEMS motion sensors such as accelerometers, gyroscopes, digital compasses and inertial modules, they have become an important part

of wearable electronics devices. With accelerometer data, walking and running parameters; with gyroscope data motion orientation; with GNSS module position and velocity; with barometers altitude information can be obtained. Although wearable electronic devices with MEMS sensors can provide various parameters related to motion and offer promising alternative for optical motion tracking systems, there are several points that should be considered

- Motion tracking for outdoor environments cannot be implemented by stand-alone GNSS systems due to relatively low update rate of GNSS system. Data update rate of commercial grade GNSS modules are around 5Hz and for human motion tracking applications, high speed motion should be monitored. Motion tracking solutions for sports applications have sampling rate at least 10Hz, typically 50-200Hz. Therefore, integration of inertial system and high precision GNSS system for outdoor motion tracking is required.
- For indoor environments where GNSS signals are not available, parameter related to motion such as velocity should be provided together with inertial measurement unit data by a means of aiding system rather than GNSS to have accurate estimation of movement. Ultrawide band technology offers promising alternative for GNSS in indoor environments due to its high accuracy localization feature. However, it is not yet employed in contemporary motion tracking applications.
- To capture high dynamics of human motion with reasonable accuracies, inherent errors of MEMS sensors should be minimized.

The goal of this thesis to make contribution into development of small inexpensive motion trackers that can be alternative to optical motion tracking systems. The developed motion tracking algorithms have been tested on a prototype that integrates inertial measurement unit, GNSS receiver and ultrawide band radio system and data post-processing algorithm. Ultimately, reasonable accuracies in movement tracking for indoor and outdoor are expected. The thesis gives detailed analysis of motion tracking technologies, observe the applicability of those systems together by experimenting with on shelf products and have a contribution to data processing algorithm in the project.

My tasks in data processing in MATLAB can be summarized as follows

- Recording and analyzing output data of inertial measurement unit to estimate attitude errors during stationary periods and compute velocity.
- Correction of velocity with velocity updates for stationary periods.
- Offering algorithm of velocity update for inertial measurement unit with the aid of GNSS and Ultrawide band radio.

My tasks in the analysis of human motion technologies can be summarized as follows

- Literature survey for working principles of inertial measurement units.
- Conducting experiments with Xsens IMU unit.
- Experimenting with off the shelf ultrawide band systems to measure their accuracy in terms of position and velocity.

2. HUMAN MOTION TRACKING METHODS

2.1 CHARACTERISTICS OF HUMAN GAIT

Gait cycle is generated with the help of joints which provide movement and with muscles which provide force for movement. Gait cycle repeats continuously with distinguishable pattern as subject walks or runs. Medical professionals or physiotherapists analyze gait cycle after subject walks or runs on treadmill. Gait cycle is characterized by several phases such as heel push off, swing, heel strike and stance. The stance phase is the period where the foot is in contact with the ground and the swing phases makes up the remaining cycle. After heel push off phase, swing phase starts and similarly after heel strike, stance phase starts.

Gait cycle phases for walking are shown in Figure 1
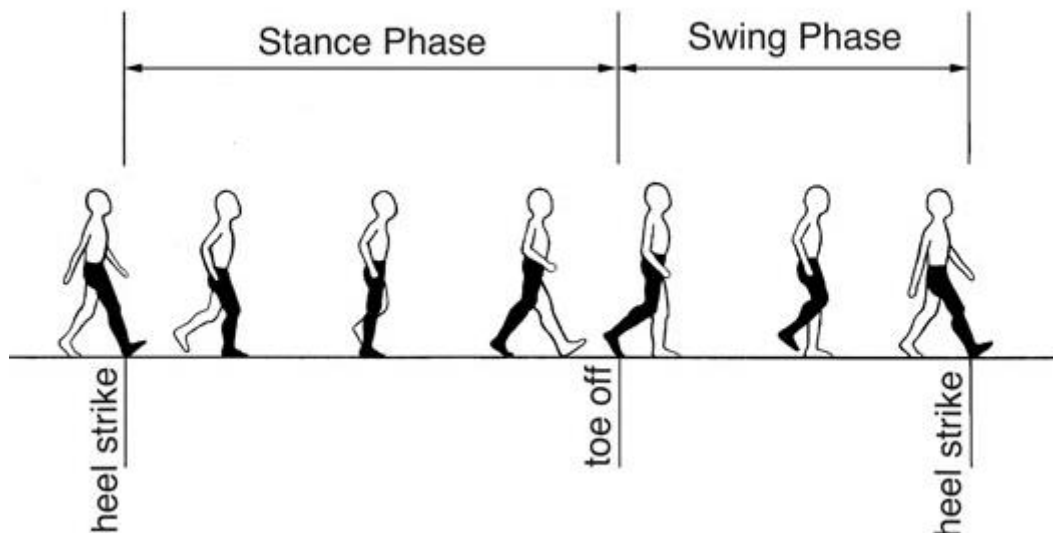
Figure 1. Gait cycle phases for walking.

According to Sidney, Gerard and Elizabeth [7] approximate time durations for gait cycle phases for walking and running are given in Table 1.

Phase	Walking	Running
Toe off	0.22	0.34
Swing	0.37	0.22
Heel strike	0.18	0.09
Stance	0.47	0.13

Table 1. Approximate time durations for gait cycle phases for walking and running.

By observing walking and running gaits, differences and similarities between two gaits and characteristics of accelerations are noted as [7] [8]

- In walking gait, magnitude of the dynamics are nearly same during movement and there is a symmetry between phases. In running gait, there is asymmetry between phases. The reason behind this behavior is that in walking gait, subject' legs carry same amount of weight at symmetrical time intervals.

- For walking and running gaits, there is long flat acceleration during stance phase due to the absence of movement.

- For walking gait cycle, accelerations in toe off phase and for running gait cycle accelerations in heel strike is abrupt and have large magnitude due to feet and ground impact.

- The reason for selecting forefoot accelerometer is due to the fact that accelerometer signals are very distinct between different phases. With accelerometer signal, distinguishing phases of gait cycle is easier.

- Subject's walking steps are longer compared to running steps due to fast dynamics of motion. This brings challenge for identifying steps without missing some steps. However, in step detection of fast movement, there will be more recorded samples compared to walking for analysis.

Main target of the thesis is not to evaluate gait cycle from motion data but rather to obtain accurate motion data to evaluate movement and related parameters. For example, in running, these parameters are split times, change in velocity, velocity at takeoff, velocity at impact, cadence, stride length and they are connected to the technique of particular athlete.

2.2 INERTIAL AND MAGNETIC SENSORS

In inertial navigation, accelerometers and gyroscopes provide acceleration and orientation data to calculate velocity and orientation of an object relative to known starting point. There are various types of accelerometers and gyroscopes with different operation principles [9]. Three gyroscopes and three accelerometers form an inertial measurement unit (IMU) that can track three dimensional rotational and translational movements. Gyro and IMU accuracy can be classified into performance grades as consumer, tactical and

navigational grades. The lowest grade is used for consumer products and highest performing grades is used for aircraft and submarine navigation. The accuracy of the sensors is roughly proportional to the sensor price. Therefore, the consumer grade sensors are targeted in current work.

2.2.1 GYROSCOPES

Gyroscope data gives object's attitude in terms of rotational rates or actual turn angles. Output of rate gyros is relative to angular speed and output of rate integrating gyros is actual turn angle or heading. There are mainly 3 types of gyroscopes- mechanical, optical and MEMS. Detailed operation principles of different type of gyroscopes are presented in [9]. Comparison of mechanical, optical and MEMS is presented in Table 2.

	Advantages	Disadvantages
Mechanical	• Wide performance range • Low noise	• Relatively high cost • Long warm up • Fragile to friction and output drift
Optical	• Rapid reaction on turn on • Rugged (no moving parts)	• RLG is high voltage device • FOG is temperature sensitive
MEMS	• Very small and low weight • Low cost • No moving parts • Rugged • Short start up time • Inexpensive to produce in high volume • Compatible with operations in hostile environments • High reliability	Still under development for higher precision

Table 2. Advantages and disadvantages of mechanical, optical and MEMS gyroscopes.

Drawback of standalone gyroscopes is that their angular turn angle output drifts with time due to integration errors. Integration process is sensitive to deterministic and stochastic errors that will be explained in chapter and section 2.2.4

2.2.2 ACCELEROMETERS

An accelerometer is a device that measures translational acceleration resulting from the forces acting on it. There are three types of accelerometers mechanical accelerometers, solid state accelerometers and MEMS accelerometers. Mechanical accelerometers consists of mass, spring and displacement pick-off and measures forces acting on mass to measure accelerations. Solid state accelerometers consists of cantilever beam, mass and they are surface acoustic wave, vibratory, silicon and quartz devices. Accelerations are measured from frequency changes. MEMS accelerometers uses piezoelectric effect for sensing accelerations. Interested reader can refer to [9] for detailed operation principle of different type of accelerometers. MEMS accelerometers have even bigger movement measurement error due to need of double integration and accumulation of nonlinearities.

2.2.3 MAGNETOMETERS

Angular rate and angular angle data from gyroscopes can provide attitude information. However, due to inevitable gyroscope and accelerometer drifts mentioned above, attitude errors increase with the time. One solution for attitude error mitigation is to use magnetometers as an external aiding source for orientation that does not exhibit unlimited error accumulation. A three dimensional measures the vector of the earth's magnetic field. Horizontal components of the magnetic field are used to determine magnetic north, which differs from true north. The difference is called magnetic declination that should be corrected to obtain true north [10]. Magnetic declination depends on geographical latitude and longitude and day of the year. A prediction of current magnetic declination for a given location can be obtained online from the publicly available databases.

Although, magnetometers can provide compensation for errors, there are several disadvantages of magnetometers. Firstly, they are affected by local disturbances in the earth's magnetic field caused by nearby ferrous magnetic objects. The ferrous materials will distort, or bend, the magnetic field therefore effects of magnetic disturbances should be considered during calibration phase of magnetometers [10]. Secondly, magnetometers

do not provide absolute correction for gyroscope errors [11]. Lastly, magnetic field should be strong for harsh environment and field strength is not constant due to disturbances [12].

2.2.4 MEASUREMENT ERRORS OF MEMS ACCELEROMETER AND GYROSCOPES

Accelerometers and gyroscopes errors are categorized as deterministic and stochastic errors. Deterministic errors of gyroscopes and accelerometers can be precisely determined and their behavior can be mathematically modelled. *Constant bias*, *scale factor errors and misalignment error* are in this category. On the other hand, stochastic error's behavior is based on random process meaning that exact value of a specific error term will be different at any different time instances. *Measurement noise* and *bias instability* are in this category [13]. In order to have accurate heading and velocity information, either high accuracy and expensive gyroscopes and accelerometers should be used or effects of sensor errors should be compensated.

Constant bias, also called drift and offset error, is the output of gyroscope or accelerometer when it is not undergoing any rotation (zero input). Constant bias errors of gyroscopes and accelerometers for different grades of sensors are compared in the Table 3 [14].

Error/ type of sensor	Navigation grade	Tactical grade	Consumer grade
Gyroscope bias	0.005-0.01 deg/h	1-10 deg/h	More than 100 deg/h
Accelerometer bias	10-50 µg	100-500 µg	1-20 mg

Table 3. Constant bias errors of gyroscopes and accelerometers for different grades of sensors.

The constant bias error of a rate gyro and accelerometer can be estimated by taking a long term average of the gyro's output when it is not undergoing any rotation.

To find constant bias errors of the accelerometer and gyroscopes of Xsens IMU, half an hour IMU data is collected at 600Hz and mean values of constant bias of gyroscope and accelerometer are found. Figure 2 and 3 shows x and y axis gyroscope and accelerometer constant bias with respect to measurement points respectively.
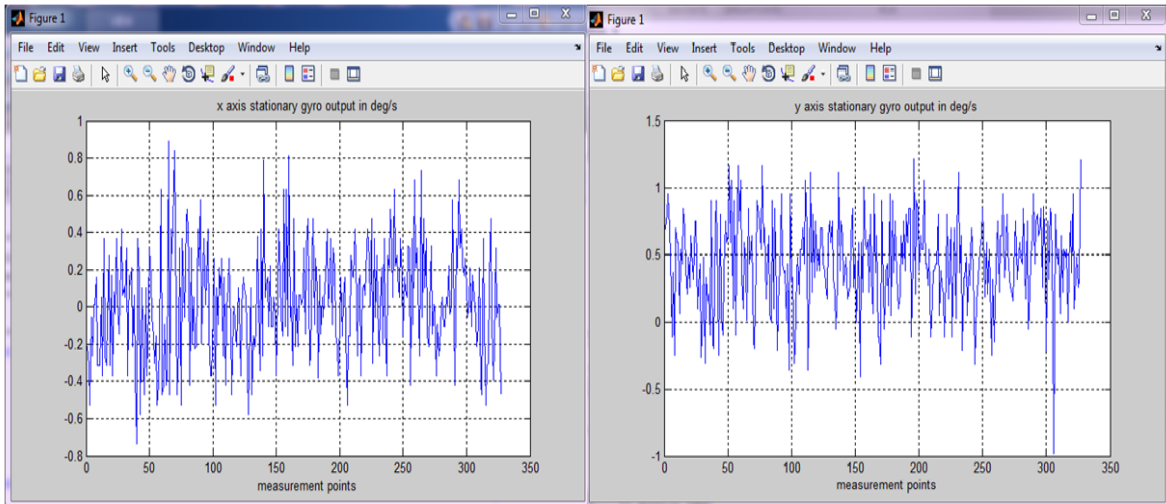
Figure 2. X and y axis gyroscope constant bias with respect to measurement points.
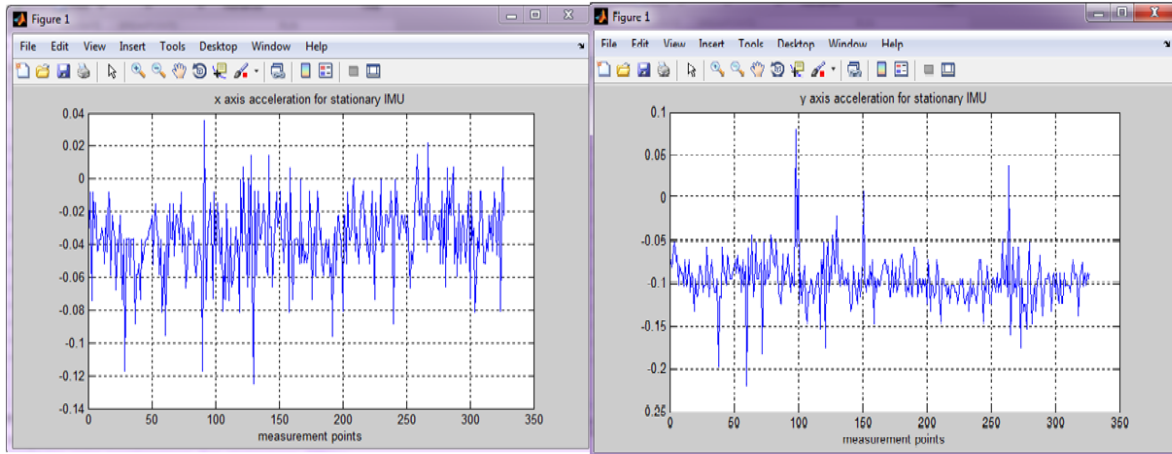
Figure 3. X and y axis accelerometer constant bias with respect to measurement points.

Table 4 shows mean values of x and y axis constant bias values for gyroscope and accelerometer in Xsens IMU

	Gyroscope	Accelerometer
x axis bias	92 degree/h	3.6 mg
y axis bias	1560 degree/h	9.8 mg

Table 4. X and y axis constant bias values for gyroscope and accelerometer of IMU.

Comparing Table 4 with Table 3, it is possible to consider the grade of Xsens MTw IMU between tactical and consumer grade.

Scale factor errors offset data by a multiplicative constant. It relates the change in the output signal to a change in the measured input rate. Scale factor errors of gyroscopes and accelerometers for different grades sensors are compared in the Table 5 [14]

Error/ type of sensor	Navigation grade	Tactical grade	Consumer grade
Gyroscope scale factor error	10-50 ppm	100-300 ppm	1-3%
Accelerometer scale factor error	10-50 ppm	100-300 ppm	1-3%

Table 5. Scale factor errors of gyroscopes and accelerometers for different grades sensors.

Since MEMs sensors are sensitive to temperature, temperature can drift both static biases and scale factor errors. For each temperature, static biases and scale factor errors are different therefore instead of modelling errors with single values, errors must be modeled as a series of matrix pairs arranged in a look-up table based on temperature. In order to compensate effects of temperature, IMU are calibrated within operation temperature [13]. Temperature operation range of Xsens MTw IMU is reported as 0°C-55°C. Bias instability, also called turn on to turn off bias, indicates the difference between static bias values for different data collection or power cycle of sensors. It can be modeled as a stationary Gauss-Markov stochastic process. Measurement noise is random process and it is modelled according to its power spectral density (PSD) and its probability distribution function (PDF). Gaussian distributed probability density function is preferred due to its suitability to natural occurring events and its simplicity for mathematical operations [13]. In order to evaluate performance of accelerometer and gyroscopes, resolution and non-linearity specifications should be considered. Resolution is defined as smallest detectable increment in accelerations and angular rates. Angular resolution of Xsens IMU are given as 0.05 degree.

Values for bandwidth and noise power spectral density of accelerometer and gyroscope in Xsens IMU are given in Table 6 [15]

	Accelerometer	Gyroscope
Analog bandwidth	120Hz	140Hz
Noise power spectral density	0.003 m/s^2/√Hz	0.05 deg/s/√Hz

Table 6. Bandwidth and noise power spectral density of accelerometer and gyroscope in Xsens IMU.

Non linearity of sensor indicate non linearity input and output relationship of the sensor and defined as

Non linearity= (maximum deviation / full scale output) x 100%

Values for Full scale output and non-linearity of accelerometer and gyroscope in Xsens IMU are given in Table 7 [15]

	Accelerometer	Gyroscope
Full scale	±160 m/s^2	±1200 deg/s
Linearity	0.2%	0.1%

Table 7. Full scale output and non-linearity of accelerometer and gyroscope in Xsens IMU.

2.3 INERTIAL MEASUREMENT UNITS

In inertial navigation systems, accelerometer measurements are used to calculate velocity and position during movement. In order to define frame where acceleration takes place, gyroscopes constantly determine orientations of acceleration and hence velocities. With this knowledge, orientation, position and velocity of moving object can be tracked relative to initial position. Advantages of inertial navigation is that since it is autonomous, it does not rely on any external aids or on visibility conditions and it is immune to jamming. On the other hand, it is prone to errors in longer time durations and it brings acquisition cost, operation cost and maintenance cost [16].

IMUs consist of three axis accelerometers and gyroscopes at three perpendicular axis. It brings 6 degree of freedom because movement and rotation along the three axis are independent of each other.

Gait analysis in the chapter and section 2.1 together with accelerometer data from IMU can be used to estimate parameters related to walking and running. Firstly, accelerometer data coming from body mounted accelerometers can be used to estimate time of step occurrence. Secondly, if total number of steps can be estimated correctly, travelled distance of subject can be estimated by multiplying step size with number of steps. In fact, together with travelled distance and heading information, the distance and direction of steps can be estimated [12].

Step detection algorithms and heading estimations are main elements in pedestrian dead reckoning systems (PDR) [12]. In pedestrian dead reckoning systems, accelerometer data is used in step detection and gyroscopes are used in heading estimation. By knowing initial position, attitude and step size occurrences and heading during movement, subjects can be tracked. Figure 4 shows complete block of pedestrian dead reckoning systems.
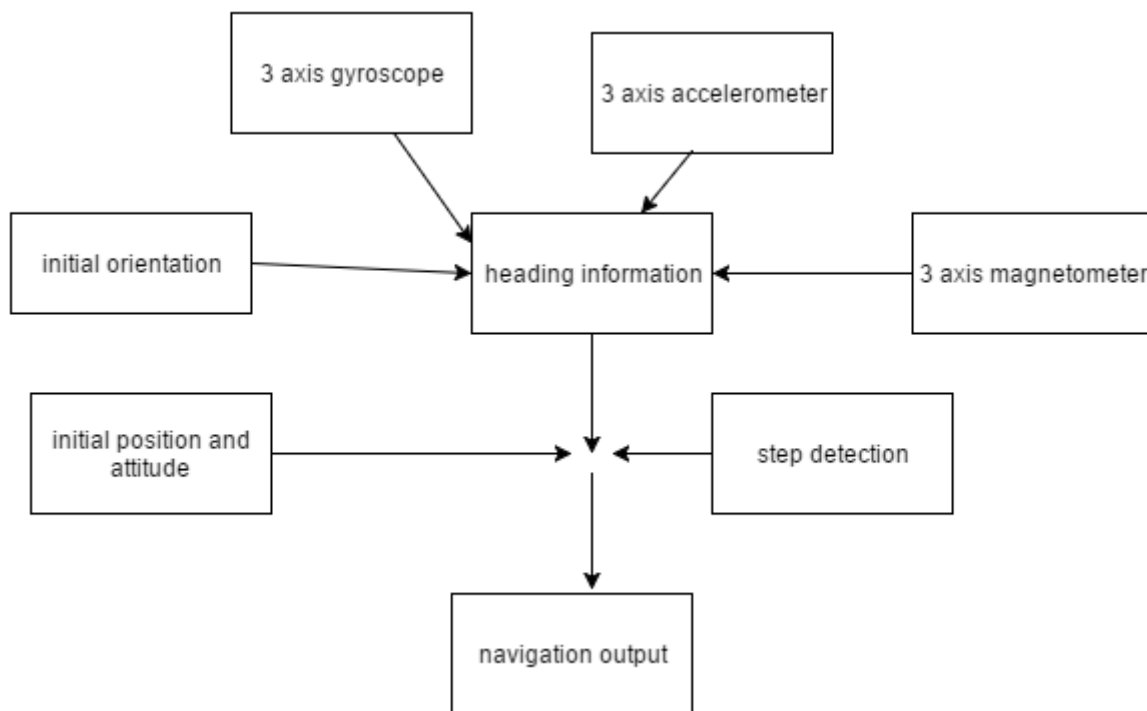
Figure 4. Block diagram of a pedestrian dead reckoning systems.

Inertial measurement units are classified according to navigation frame where output of data is measured. If output is measured in the body frame and accelerometer signals are converted to global frame using orientation information, the system is called strap down system. Another inertial measurement unit is called stable platform system and interested reader can refer to [9] for detailed information about stable platform systems. The measurement unit that I used in my experiments is strap down type unit therefor main focus will be on strap down system.

2.3.1 XSENS MTw IMU

Wireless motion tracker that i used in my experiments is MTw from Xsens technologies. MTw miniature lightweight (34.5 mm x 57.8 mm x 14.5 mm, weight 27 g), LiPo battery powered wireless inertial measurement unit incorporating 3D accelerometers, gyroscopes, magnetometers (3D compass), a barometer (pressure sensor for altitude measurement.

Hardware part of system consists of MTw, Awinda master, awinda station, awinda usb dongle and MTw body straps. Figure 5 shows all hardware system components [17]

Figure 5. Hardware system components of MTw [17].

Awinda master serves interface between MTw's and display unit (computer with Xsens based software) and synchronize data from MTw's. 20 simultaneous MTw's can be connected and maximum range is 50m [15]. Awinda USB dongle has similar function as awinda master except its range is shorter. Awinda station charges up to 6 MTw's simultaneously and controls the reception of synchronized wireless data from all wirelessly connected MTw's [17]. The body straps allow MTw's to be worn. During my experiments, I only used MTw and USB dongle since, one MTw is needed at a time.

Software part of system is either MT Manager, the standard logging and visualization tool from Xsens or a self-built program based on Xsens software development kit (SDK). MT manager functionalities are displaying of 3D orientation, inertial and magnetic data, creating log files of data as .mtb files and exporting .mtb log files to .txt format.

Data transfer between Xsens MTw IMU and display unit is realized wirelessly using Bluetooth technology. It is based on IEEE 802.15.4 physical layer (PHY), 2.4 GHz chipsets which operates in ISM (industrial Scientific Medical) band.

It is possible to choose data rate-sampling time (Hz) and channel number during wireless network setup with wireless configuration tab in MT manager. Wireless configuration is used to initialize communication between Master station and MTw's and after wireless connection is set up, Master station ID, MTw IDs and received signal strength appears on screen. Figure 6 shows example of wireless configuration screen for the MTw and master station that i used in my experiments.
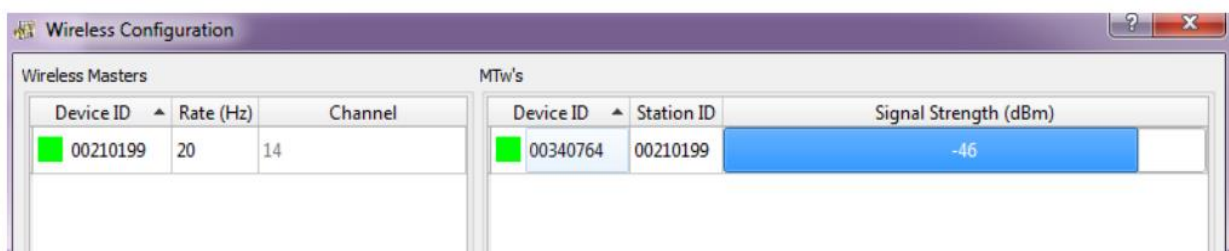
Figure 6. Wireless configuration screen for the MTw and master station.

Since data transfer from MTw to display unit is implemented wirelessly, this feature is cable-free which gives freedom of movement and make it suitable for motion tracking applications.

2.3.2 COORDINATE SYSTEM OF IMU
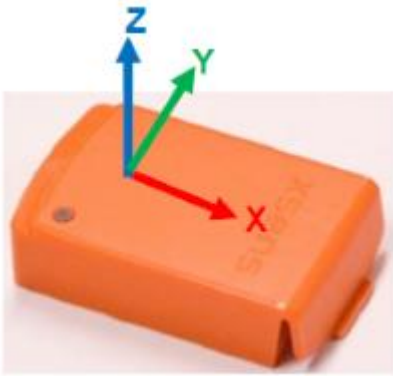
Coordinate system of the unit is defined with respect to the local north where positive x axis point's local magnetic north, y axis point's west direction and z axis points up direction. Figure shows coordinate system of the unit. Figure 7 shows the MTw unit with sensor axes.

Figure 7. Sensor axis of MTw [17].

Acceleration data coming from the unit are in its axis which is body axes.

2.3.3 OUTPUT DATA OF IMU

Since output of sensors are in body frame, measurement data should be converted to global frame by coordinate transformations. There are three different type of coordinate transformations such as Euler angles, direct cosine matrix and quaternions.

Euler angles represent coordinate transformations in terms of angular rotations. They are referred as roll, pitch and yaw angles. Roll, also known as bank, angle (Φ) axis is defined as rotation around x axis in range -180° and +180°. The pitch, also known as elevation and tilt, angle (θ) is defined as rotation around y axis in range -90° and +90°. The yaw (also known as heading) angle (Ψ) is defined as rotation around z axis in range -180° and +180°. Figure 8 shows Euler angles
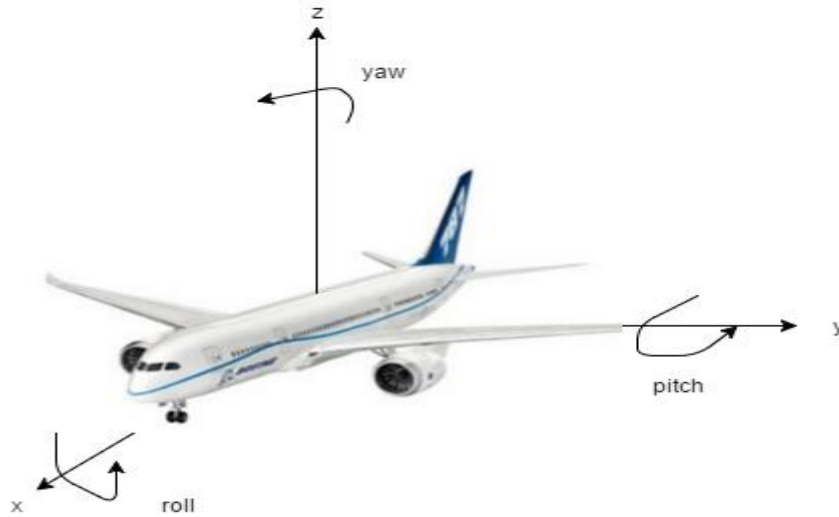
Figure 8. Euler angles.

Rotation matrix is used to convert arbitrary uvw coordinate frame to xyz coordinate system or vice versa. Set of conversions are expressed in rotation matrices. Each pitch, roll and yaw angles have their own rotations and expressed in $R_\theta{}^Y$, $R_\Phi{}^X$ and $R_\Psi{}^Z$ respectively.

$$R_\theta^Y = \begin{bmatrix} cos\theta & 0 & sin\theta \\ 0 & 1 & 0 \\ -sin\theta & 0 & cos\theta \end{bmatrix} \qquad R_\Phi^X = \begin{bmatrix} 1 & 0 & 0 \\ 0 & cos\Phi & -sin\Phi \\ 0 & sin\Phi & cos\Phi \end{bmatrix} \qquad R_\Psi^Z = \begin{bmatrix} cos\Psi & -sin\Psi & 0 \\ sin\Psi & cos\Psi & 0 \\ 0 & 0 & 1 \end{bmatrix}$$

To have one rotational matrix (R_{GS}) that incorporates all rotations of pitch, roll and yaw angles with respect to xyz coordinate, individual rotation matrices are multiplied.

$$R_{GS} = \begin{bmatrix} cos\Psi & -sin\Psi & 0 \\ sin\Psi & cos\Psi & 0 \\ 0 & 0 & 1 \end{bmatrix} \begin{bmatrix} cos\theta & 0 & sin\theta \\ 0 & 1 & 0 \\ -sin\theta & 0 & cos\theta \end{bmatrix} \begin{bmatrix} 1 & 0 & 0 \\ 0 & cos\Phi & -sin\Phi \\ 0 & sin\Phi & cos\Phi \end{bmatrix}$$

The rotation matrix (R_{GS}) is multiplied by the measured accelerations in the x, y, and z in body frame to obtain the accelerations in the x, y, and z global reference coordinate frame. In chapter and section 3.2.4, i used direct cosine matrix multiplication with body frame acceleration to obtain accelerations in global from and velocity in global frame.

Quaternion orientation output represents a rotation about a unit vector n through an angle α and is denoted as q_{GS} = (q_0, q1, q2, q3). It similarly rotates vector in body frame to global reference coordinate frame as direct cosine matrix.

Conversation equations between Euler angles, direct cosine matrix and quaternion can be found in reference [17]. During my experiments, i used built in MATLAB functions such as quat2angle, angle2quat, quat2dcm, angle2dcm for conversion whenever it is needed.

In MT Manager Preferences tab, it is possible to select output orientation format as Euler angles quaternions or direct cosine matrix. With ASCII exporter, log files can be converted to .txt format for further processing. Converted sample .txt file in Euler angles format in excel looks like in Figure 9

1	// Start Time: Unknown																
2	// Update Rate: 120.0Hz																
3	// Filter Profile: human (34.3)																
4	// Firmware Version: 1.0.10																
5	PacketCou	SampleTir	Acc_X	Acc_Y	Acc_Z	Gyr_X	Gyr_Y	Gyr_Z	VelInc_X	VelInc_Y	VelInc_Z	OriInc_q0	OriInc_q1	OriInc_q2	OriInc_q3	Roll	Pitch	Yaw
6	45458	0	0.170967	-0.146502	10.143.916	0.005035	-0.021515	0.002518	0.001417	-0.001223	0.084533	0.999999	0.000021	-0.000090	0.000010	-0.828620	-0.960352	0.993118

Figure 9. Euler angle output data of MTw in .txt format in Excel.

Packet counter in first column indicates time instances where measurement samples are taken. By knowing first and last packet counter number and by using sampling frequency, recording time of data can be obtained by

measurement_time= (last value of packet counter- first value of packet counter) /sampling frequency

Explanations of each column of IMU output data is as follows

- Acc_X, Acc_Y, Acc_Z indicate acceleration in m/s^2 in x, y and z sensor axis respectively (body frame)
- Gyr_X, Gyr_Y, Gyr_Z indicate angular rate in radian/s in x, y and z respectively
- VelInc_X, VelInc_Y, VelInc_Z indicate velocity increment in m/s and they are output of SDI block
- OriInc_q0 is real component of orientation increment quaternion and output of SDI block
- OriInc_q1, OriInc_q2, OriInc_q3 indicate orientation increment quaternion in x, y, z axis respectively and output of SDI block
- Roll, pitch, yaw indicate orientation in degree with respect to fixed coordinate system

26

Similarly, sample .txt file in direct cosine matrix format in excel looks like in Figure 10

VelInc_X	VelInc_Y	VelInc_Z	OriInc_q0	OriInc_q1	OriInc_q2	OriInc_q3	Mat[1][1]	Mat[2][1]	Mat[3][1]	Mat[1][2]	Mat[2][2]	Mat[3][2]	Mat[1][3]	Mat[2][3]	Mat[3][3]
-0.000549	-0.001465	0.081970	0.999999	0.000027	0.000028	0.000023	0.999838	-0.017527	0.004137	0.017523	0.999846	0.001037	-0.004155	-0.000964	0.999991
-0.000432	-0.001461	0.081725	0.999999	0.000035	-0.000002	-0.000023	0.999837	-0.017560	0.004142	0.017556	0.999845	0.001107	-0.004161	-0.001034	0.999991

Figure 10. Direct cosine matrix output data of MTw in .txt format in Excel.

2.3.4 MISALIGNMENT CORRECTION

Since acceleration output of IMU is in body frame, converting body frame accelerations to global frame by using direct cosine matrix is necessary to obtain velocity in global frame. After velocities in global frame are found, they should be updated periodically to minimize misalignment errors of IMU. Misalignment errors occurs when default sensor axis are not properly aligned with axis defined by inertial measurement unit. Axis of IMU are defined by unit vectors that are perpendicular to faces of the IMU and if one sensor axis is not aligned with axis of IMU, additional accelerations and angular velocities that occur in other two axis accumulates on this axis. Figure 11 shows misalignment between Y axis of IMU and y axis of sensor.
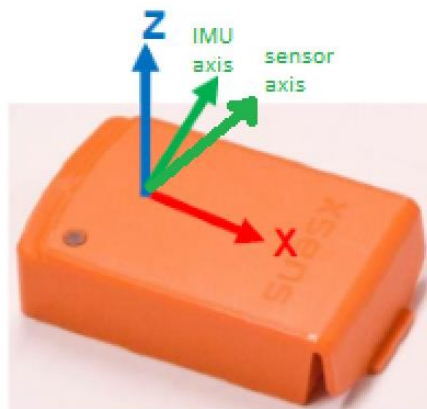
Figure 11. Example misalignment in y axis of IMU.

Velocity errors in x and y direction are linked to misalignment angles as

$$\Delta Vx = -g \times \Delta \varphi \times \Delta T \qquad (1)$$
$$\Delta Vy = -g \times \Delta \theta \times \Delta T \qquad (2)$$

where

ΔVx and ΔVy are velocity error in x and y axis respectively (m/s)

g is gravity of earth (9.8 m/s^2)

$\Delta \varphi$ and $\Delta \theta$ are roll angle and pitch misalignment angles respectively (radians)

ΔT is time duration in which velocity error grows (s)

The algorithm for velocity correction was in MATLAB. The software takes raw accelerations from stationary IMU at 120Hz sampling rate during one minute, converts them into global accelerations and calculates x and y axis velocities in global frame. After velocities are computed in global frame, the velocity update is implemented. Since IMU is held stationary, it is known that velocity output should be zero. However, due to misalignment, velocity grows linearly with time. With the code above, data points are divided into segments and for each segment, deviation from true velocity (for stationary IMU, it is zero) is calculated. By knowledge of deviation of each segment from true velocity, misalignment roll and pitch angles are calculated according to formula (1) and (2). As a final step, initial direct cosine matrix which is obtained from Euler angles of IMU output are corrected for each segment. Velocities are obtained from accelerations from built-in matlab function cumtrapz. Interested reader can refer to Appendices 1 for the code segment. Figure 12 shows sample velocity output without velocity update and with velocity update of 5 seconds for stationary IMU for x and y axis. Red line shows velocity without correction and blue line shows velocity with correction.
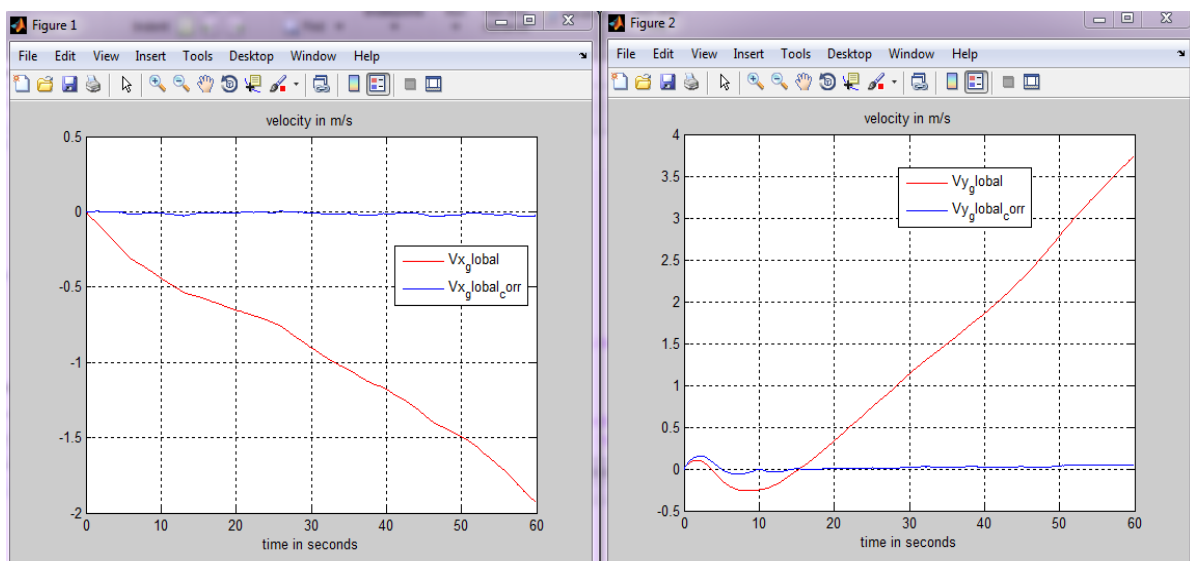
Figure 12. Stationary velocity output of IMU without velocity update and with velocity update of 5 seconds

Figure 13 shows sample velocity output without velocity update and with velocity update of 30 seconds for stationary IMU. Red line shows velocity without correction and blue line shows velocity with correction.
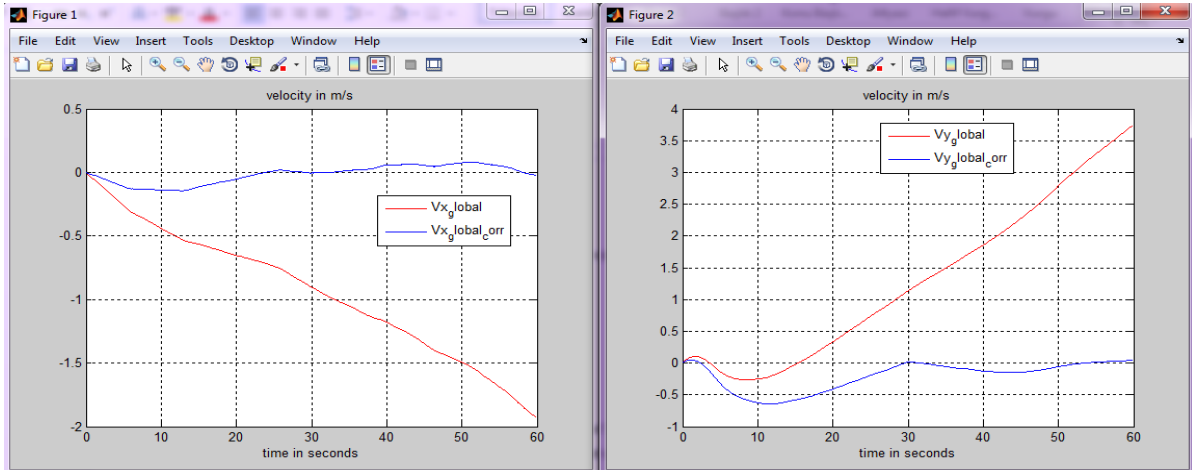
Figure 13. Stationary velocity output of IMU without velocity update and with velocity update of 30 seconds

With velocity update of 5seconds maximum velocity error is 0.04 m/s and 0.15 m/s for x and y axis velocities respectively. With velocity update of 30 seconds maximum velocity error is 0.08 m/s and 0.64 m/s for x and y axis velocities respectively. However, without velocity update, velocity error grows almost linearly with 0.03 m/s per second and 0.06 m/s per second for x and y axis velocities respectively.

To estimate running, walking performance, accuracy targets in velocity should be between 0.02-0.05 m/s with 100 Hz update. Most critical element is misalignment correction to achieve the accuracy target since other sensors errors explained in chapter 2.2.4 are mostly factory calibrated. As the update frequency of misalignment correction through velocity increases, velocity accuracy increases. Therefore, misalignment procedure explained in 2.3.4 for stationary IMU should be extended for real motion where knowledge of zero velocity output is no longer valid. For real motion, IMU velocity output should be updated with other complementary velocity source.

3. LOCALIZATION METHODS

As experiments show in chapter and section 2.3.4, velocity output accuracy depends on update frequency of misalignment correction through velocity. To achieve accuracy target in human velocity measurements, complementary source should provide velocity or position data to IMU sensor as frequently as possible and with minimum bias. With the use of high accuracy localization sources as a complementary source and misalignment correction, accuracy target in velocity can be achieved for real dynamic motion.

For outdoor environments, high precision GNSS systems can provide both velocity and position at 5Hz with accuracies 0.1m/s and 1m for velocity and position respectively. Therefore, high precision GNSS systems in motion tracking for outdoor environments as a complementary source is the best selection. For indoor environments, there is usually no direct line of sight to satellites in sky and construction materials of buildings such as brick, metal attenuate signals. Indoor positioning technologies are being developed to overcome limitation of GNSS system such as RSSI based WLAN fingerprinting, ultrasound and ultra wideband radio time of flight (ToF) or Doppler effect based measurements. UWB as ToF based technique has advantage of better positioning accuracy, shorter setup time and higher operation range compared to RSSI based WLAN fingerprinting and has advantage of multipath tolerance and fast propagation of radio signals compared to ultrasound [4]. Moreover, convenient hardware implementation of ultrawide band with inertial system and GNSS receiver in data logger makes ultrawide band ideal candidate in motion tracking for indoor. Interested reader can refer to [4] for operation principles and details for RSSI based WLAN fingerprinting and ultrasound. In the following sub chapters, high precision GNSS and Ultrawide band are explored as possible source of the update of IMU velocity for outdoor environments and indoor environments respectively.

3.1 HIGH PRECISION GNSS

Satellite navigation has been used extensively over years ranging from tracking systems, pedestrian navigation systems, intelligent transportation systems, aircraft approach and landing, navigation of agricultural machineries. As new systems and applications emerged, there is a demand for improved performance parameters of GNSS systems such as accuracy, availability, integrity and continuity. With high performance systems,

accuracy provides navigation output not to deviate from true position and stay in acceptable error range; integrity provides warning to user in the case of positioning solution is not trustworthy; continuity provides navigation solution to be accurate for duration of intended operation time; availability provides ability of the system to be used whenever it is required [18]. Main factors affecting the accuracy of navigation output can be summarized as

- Satellite orbit and clock errors
- Ionosphere conditions
- Multipath propagation
- Radio Frequency interference

Information of exact position of satellites in constellation is prerequisite for trilateration by which distance of user to satellites in view are measured by arrival time of signals to user. High precision atomic clocks of satellites and stable satellite orbits make triangular solution possible. Satellites are observed and controlled by ground control station which updates navigation message broadcasted by satellites. Navigation message is specific for each satellite and includes ephemeris parameters by which user receiver can calculate position of corresponding satellite. Satellite position, velocity and clock parameters (phase bias, frequency bias and drift rate) are determined by prediction model of ground control station. Errors related to satellite orbit prediction and clock comes from estimation of current state and prediction of future values. Typical rms errors due to ephemeris and clock parameters are 1m for each and depends on update rate of navigation message by control segment.

Another factor affecting positioning accuracy is properties of propagation environment. When the signal travels from Medium Earth orbit (MEO) satellite to user, it is affected by ionosphere. Short term unpredicted effects solar activity and magnetic disturbances causes variability within ionosphere causes delays and advances code phase and carrier phase measurements respectively. Therefore, depending on condition on ionosphere and path length of signal through ionosphere brings positioning error typically 5m and most dominant source of GNSS errors. In order to mitigate ionosphere errors, new civilian signals at different frequencies will be used in GNSS modernization. L5 signal at 1.176.45 MHz are added to GPS frequencies. Dual frequency receivers can obtain ionospheric free pseudo range by measuring two different measurements at two different frequencies.

Since received signals are weak, GNSS signals are vulnerable to radio frequency interface in the form of jamming and spoofing. Depending on interference power level, positioning solution degrades from true position. Finally, multipath propagation causes reflected signals to be received by user and this brings degradation of positioning solution on the order of 0.5m-1m depending on satellite elevation angle [19].

Due to error sources and in order to mitigate positioning errors for better availability, integrity and continuity, several augmentation systems and additional ranging facilities are used in GNSS systems such as

- Satellite based augmentation systems (SBAS)
- Differential GPS (DGPS)
- Ground based augmentation systems (GBAS)
- Multi-GNSS systems

Satellite based augmentation (SBAS) systems consists of ground segment reference stations spreaded over continental areas with known locations; master control center which generates wide area correction message according to processed data; navigation Land Earth stations which up links messages to geo-stationary (GEO) satellites. In SBAS operation, reference stations measures code phase and carrier phase measurements from all visible satellites and according to these measurements, master station calculates clock and ephemeris corrections together with error bounds for ionospheric corrections. Correction parameters are transmitted by land earth stations to GEO satellites and linking down to user receivers. Finally user receivers apply best corrections available to initial measurements according to signal coming from GEO satellites. Broadcasted signal from GEO satellites are in L1 band of GPS with the exception that 250bps modulation data rate as opposed to 50bps GPS navigation message [18].

Figure 14 shows SBAS data flow
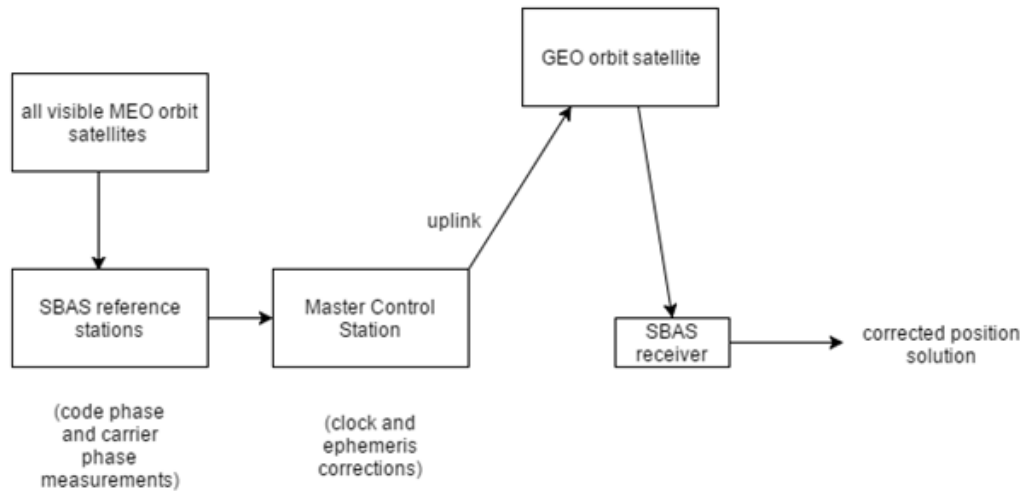
Figure 14. SBAS data flow.

Wide Area Augmentation System (WAAS) is an augmentation to Global Positioning System (GPS) for North America and Canada and operational since 2003. The European Geostationary Navigation Overlay Service (EGNOS) is developed by European Space Agency (ESA) to complement the GNSS systems since 2009. It provides open service for pedestrian, car navigation; safety of life service for aviation and maritime. Similar to the WAAS and EGNOS, the Japanese MTSAT Satellite-Based Augmentation System (MSAS), Russian System for Differential Corrections and Monitoring (SDCM) and Indian GPS Aided GEO Augmented Navigation (GAGAN) are used for augmentation. Satellite based augmentation systems are also called Wide Area Differential GPS since the operation principle is same as DGPS with the exception that correction parameters are broadcasted for larger geographical areas with GEO satellites. As in DGPS systems, coverage of reference station is smaller and the transmission of the correctional data is realized with either terrestrial radio signals, mobile communication systems.

In contrast to SBAS, Ground based augmentation systems (GBAS) is used in aviation and consists of small number of reference stations at airports and correction and error bounds are transmitted to aircrafts VHF data broadcasting from host airport with update rate of 0.5s [20]. Multi-GNSS systems can select signals from different GNSS system

constellations and better positioning accuracies can be obtained with the cost of complexity at front ends of receivers and processing power.

GNSS module used in the project is U blox Neo-7P which uses available SBAS satellites and if the service is made available, the receiver is capable of receiving signals from different SBAS systems in parallel. It chooses best SBAS satellite and the sets DGPS flag in the receiver's output control messages. Ionosphere correction improvement by using SBAS feature enables 2m horizontal positioning accuracies. Positioning accuracy is 2.5m when only GPS satellites are used for positioning with update rate up to 10Hz. Velocity accuracy of 0.1m/s is also noted [21]. Figure 15 shows precise point positioning module U blox Neo-7P.

Figure 15. Ublox Neo-7P: precise point positioning module [21].

3.1.1 FUSION OF IMU AND GNSS DATA

Data logger in the project has Xsens MTw inertial measurement unit with Ublox receiver and output of data logger in .txt format contains following information

- GPS sequence number
- IMU sequence number
- GPS latitude, longitude and altitude
- IMU angular velocity on x, y and z axis (rad/s)
- IMU orientation in quaternions (q0, q1, q2, q3)
- IMU linear acceleration on x, y and z axis (m/s^2)
- North, east, down velocity from GNSS output (cm/s)

Proposed integration of IMU and GNSS with program segment in MATLAB does following

- Reading data from .txt file of data logger

- Finds data points where IMU and GNSS data is available from their sequence numbers. If there is a number in sequence field, it means that data is available and if there is NAN, it means data is not available. Since update rate of IMU is higher than GNSS, separate timeline for both system is necessary.

- Calculates direct cosine matrix from quaternion output and calculates IMU velocity in global axis. The procedure is similar to calculation of velocity in the chapter and section 2.3.4.

- Finds index of data points and corresponding time when both IMU and GNSS data is available. Duration of time intervals are the update rate of GNSS which is approximately 0.25 seconds.

- Calculates velocity increments of IMU and GNSS during time intervals.

- Compares velocity increments of IMU and GNSS at the end of each time intervals. From this comparison, misalignment angle is found by

$$|\Delta Vx \text{ IMU}- \Delta Vx \text{ GNSS}| = -g \times \Delta\varphi \times \Delta T \qquad (3)$$
$$|\Delta Vy \text{ IMU}- \Delta Vy \text{ GNSS}| = -g \times \Delta\theta \times \Delta T \qquad (4)$$

where

ΔT is time interval between two GNSS data, approximately 0.25 seconds

$\Delta Vx \text{ IMU}$ and $\Delta Vy \text{ IMU}$ are velocity increments of IMU in x and y axis respectively during ΔT (m/s)

$\Delta Vx \text{ GNSS}$ and $\Delta Vy \text{ GNSS}$ are velocity increments of GNSS in x and y axis respectively during ΔT (m/s)

g is gravity of earth (9.8 m/s^2)

$\Delta\varphi$ and $\Delta\theta$ are roll angle and pitch misalignment angles respectively (radians)

Equations (3) and (4) is similar to equations (1) and (2) except that ΔV$_{GNSS}$ values are not zero since there is a motion.

- According to misalignment angles, velocity correction is implemented. The procedure is similar to correction of velocity in the chapter and section 2.3.4. After

velocity correction, IMU velocities will not drift and velocity information from GNSS will update IMU velocity. Program is robust if GNSS data fails to arrive 0.25 seconds at intervals. If there is GNSS outliers for some reason, IMU data will be used for velocities calculation and ΔT in the equations (3) and (4) will have higher values.

3.2 ULTRA WIDE BAND RADIO BASED LOCALIZATION

UWB radio technology has been in use for military, radar and sensing applications for long period of time. After regulations were implemented the by the Federal Communications Commission (FCC), UWB technology is started to be used for data communications as well and it gained popularity due to its advantages in location and tracking applications. Firstly, high bandwidth communications have advantage of strong multipath resolving capability due to the fact that large bandwidth corresponds to high range resolution. Range resolution is formulated as v/2b where v is speed of wave and b is bandwidth. In ECC band, b=2.5GHz and range resolution is 6cm and. Secondly, UWB systems can be used in low cost, complexity and low power applications since unlike conventional radio systems in which RF mixing stages (up conversion for injecting carrier frequencies on baseband signals; down conversion for rejecting carrier frequency from modulated signals) are used, UWB systems do not require mixing stage components such as local oscillators, mixers and amplifiers. UWB transmitter produces a very short time domain pulse, which is able to propagate without the need for an additional RF (radio frequency) mixing stage [22]. Thirdly, UWB signals are immune to jamming and behave noise like signal because its power radiated density is limited to -41.3 dBm/MHz in Europe in 3.1-8.5 GHz band with 5% duty cycle up to 6GHz in order not to create interference for the other systems operating in the same band.

Fourthly, high bandwidth of uwb signals enables high data rates and alternative to existing technology for Wireless personal area networks (WPAN) and short-range, high-data-rate communications. Bandwidth and data rates are directly proportional according to Shannon's Equation. Fifthly, short time domain pulses that are used in uwb radios can bring timing precision [22]. Fively, uwb signals have material penetration capability such

as walls. I have demonstrated wall penetration capability of UWB with an experiment in chapter 3.2.3. Lastly, UWB tracked tags that are used in tacking applications are wearable due to their small size and weight [23].

Although potential of UWB systems and advantages mentioned above, there are some drawbacks too. Firstly, sampling UWB signals at nyquist rate brings difficulties due to high bandwidth of UWB signals [24]. Secondly, materials like metal and liquid can cause interferences in the UWB radio signals [23].

UWB systems are based on impulse radio (IR) concept. UWB-IR brings the advantage of low power consumption and increased battery life of the system. In impulse radio systems, information is carried by short duration pulses (chips) of the order of hundreds of picoseconds. Pulses are generated discontinuously without any carrier modulation. Consecutive pulses are sent within a time frame (T_f) which is defined by a Pseudo random (PR) time-hopping code [22]. A time-hopping (TH) code is used for determining the accurate position of a signal in dedicated time frame to decrease the chance of interference between UWB systems [22]. In UWB-IR, data is modulated by pulse position modulation (PPM) in which information is conveyed by position and/or polarity of the signals; pulse amplitude modulation (PAM) in which information signal is represented by pulses with different amplitudes; on off keying (OOK) in which if a pulse is transmitted it is interpreted as a "1" bit and the absence of a pulse is interpreted as a "0" bit.

3.2.1 UWB TRANSMITTER AND RECEIVER ARCHITECTURE

UWB transmitter consists of a pulse generator, timing circuit and oscillator. Oscillator determines repetition frequency of transmitted pulses and pulse generator is responsible for generation of desired type of pulse. Timing circuits controls timing of transmissions with time hopping code. Pulse generation can be realized by several way and reference [26] introduces step recovery diode (SRD) for pulse generation.

After transmitted signal is received and amplified with low noise amplifier (LNA), it is correlated with template waveform. Output of correlation circuitry is baseband signal processing circuit which is responsible for deciding which bits are carried by received pulses [22].

Figure 16 shows top level of transmitter and receiver
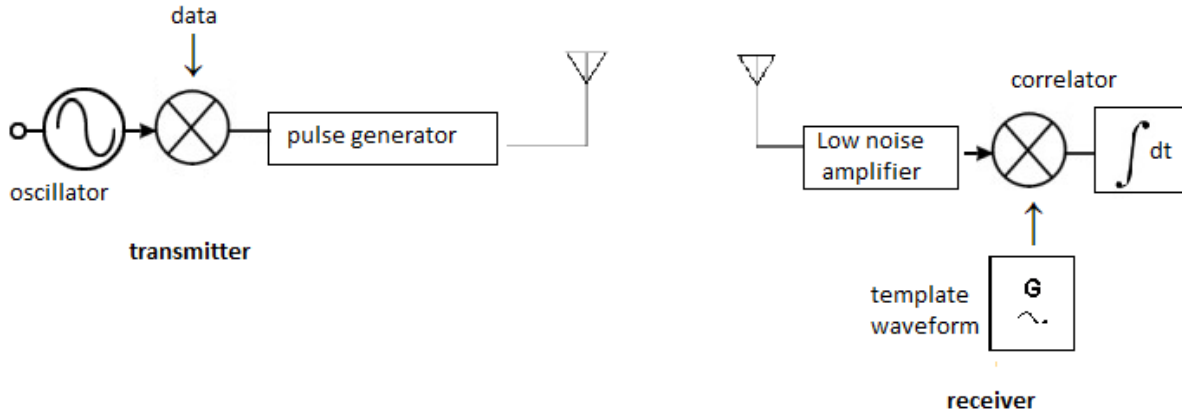
Figure 16. Top level of UWB transmitter and receiver [22].

3.2.2 UWB POSITIONING METHODS

With UWB signals, positioning of target and ranging between source and target is determined by Time of Arrival (TOA), Time Difference of Arrival (TDoA) and two way time of flight (TOF or TWR).

In TOA scheme, absolute travel time of signal from base stations (known node, transmitter, and anchor) to mobile station (receiver, tag) is measured. Measured time is given by [27]

$$T_{measured} = t_{TX} + d/c + \varepsilon_{sync}$$

Where t_{TX} denotes timestamp in the transmitter clock when the signal is transmitted, d denotes distance between source and target, c denotes propagation velocity in medium, and ε_{sync} denotes quantity that compensates any mis-synchronization between transmitter and receiver

In TDoA scheme, time differences between each signal propagation time from transmitter (base station) to receiver (mobile station) is measured. Measured time is given by [27]

$$T_{measured} = t_{TX} + d_1/c + \varepsilon_{sync} - (t_{TX} + d_2/c + \varepsilon_{sync}) = (d_1 - d_2)/c$$

Where t_{tx} denotes timestamp in the transmitter clock when the signal is transmitted, d_1 denotes distance between MS and BS1, d_2 denotes distance between MS and BS2, and c denotes propagation velocity in medium, ε_{sync} denotes quantity that compensates any mis synchronization between transmitter and receiver.

In TOF, distance between source and target is found by measuring total transaction time in which signal is transmitted to target by source, processing time (latency introduced by hardware components in source and target) in target and time of reception of signal by source. Both source and target measure time using a local clock [28] therefore positioning accuracy is highly dependent on clock oscillator offsets. After transaction time is found, distance between source and target is calculated by simply multiplying transaction time with wave propagation velocity in medium. Figure 17 shows time of flight scheme [29].
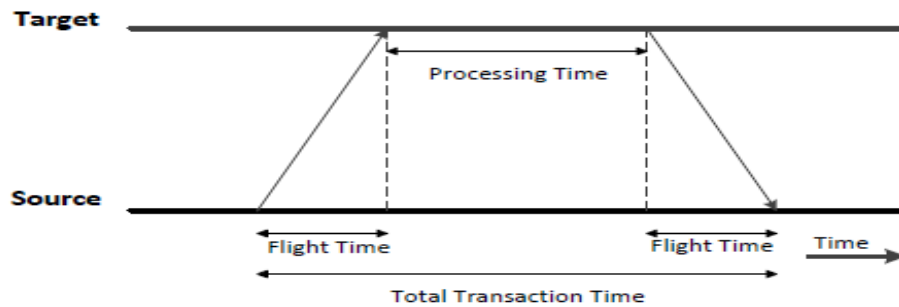
Figure 17. Time of Flight scheme [29].

3.2.3 EXPERIMENTS WITH COMMERCIAL UWB POSITIONING SYSTEMS

Centimeter level positioning accuracy is required for indoor to have velocity accuracies in the range of tens of cm/s as in high precision GNSS for outdoor. During my experiments, I used ELIKO Kio UWB system to observe if the given position and velocity accuracies are satisfied. Moreover, Bespoon system ranging accuracies are noted from the work of reference [29]. In the following subchapter, experiment results with ELIKO Kio UWB system and Bespoon are given.

3.2.3.1 BESPOON

BeSpoon devices are manufactured by BeSpoon. System consists of an Android based smartphone and 6tags. It uses UM100 module and IR-UWB type (pulse based). Operation frequency is 3-5GHz. It uses two-way time-of-flight method for ranging. Update frequency of ranging data is 4Hz. Figure 18 shows Bespoon tags and smartphone.

Figure 18. Bespoon tags and smartphone.

According to work in reference [29], line of sight and non-line of sight accuracy of the system are investigated. Line of sight test is conducted in a corridor by placing Bespoon phone on fixed location and moving a tag on different points starting from 2m to 14m with 2m steps. Non-line-of-sight (NLOS) test is conducted on corridor to investigate the effect of multipath on positioning accuracy. Seven independent measurement are taken for each distance and they are averaged. When UWB signaling is on, the phone searches for tags and when it finds a tag, tag ID and distance between tag and phone are shown. Figure 19shows LOS and NLOS corridor measurement setup.

Figure 19. Measurement setup: (a) Line of sight (b) Non line of sight.

According to tests, distance between tag and phone versus ranging error is tabulated in Table 8 for line of sight and non-line of sight measurement.

True Distance between tag and phone (in m)	Absolute Line of Sight error (in m)	Absolute Non Line of Sight error (in m)
2	0.04	0.02
4	0.01	0.07
6	0.12	0.03
8	0.01	0.12
10	0	0.27
12	0.04	0.18
14	0.18	0.13

Table 8. Line of sight and non-line of sight absolute range errors with true range, Bespoon system.

3.2.3.2 ELIKO-KIO

System consists of 4 anchors and 1tag. It uses two-way time-of-flight method for ranging. Update frequency of ranging data is 4Hz. Operation frequency is 3.1-4.8 GHz with 500MHz or 900MHz bandwidth. Figure 20 shows four anchor and a tag.

Figure 20. Eliko Kio Anchors and Tag.

Ranging data between tags and anchors can be read from any serial port terminal program. There are four anchors with IDs 413a, 413b, 413c and 409d and one tag with ID 4038.

Distance of each tag to anchor is marked with circles. Value in each circle shows distance (in cm) of anchors with ID left to it to tag. Timestamps show time (in ms) that each measurements are taken. Figure 21 shows sample output of serial port when all anchors and tag are working.
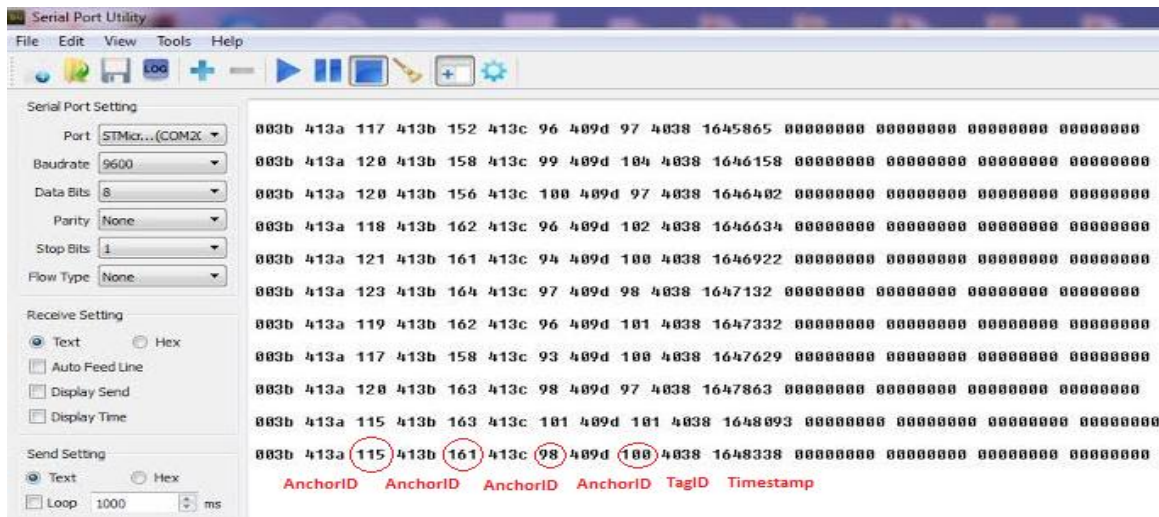
Figure 21. Sample output of serial screen.

Line of sight ranging test is conducted by placing one anchor on known position and moving tag is on straight line starting from 90cm to 990cm with 90cm steps by using simple measurement tape. Ranging data is collected from serial port program. In order to have more precise results, 10 range samples are taken and averaged. Similarly, non-line of sight ranging test is conducted by placing one anchor on known position behind concrete wall and tag is moved on straight non line path from anchor along corridor starting from 90 cm to 990 cm with 90 cm steps by using simple measurement tape. According to the measurements, true distance between the tag and the anchor versus error in measurement is plotted in Table 9 for line sight and non-line of sight.

True X,Y position of tag (in m)	Absolute Line of Sight error (in m)	Absolute X,Y errors (in m)
0.9	0.08	0.07
1.8	0.06	0.07
2.7	0.05	0.02
3.6	0.09	0.04
4.5	0.08	0.03

5.4	0.06	0.12
6.3	0.06	0.18
7.2	0.08	0.28
8.1	0.09	0.15
9	0.05	0.18
9.9	0.04	0.2

Table 9. Line of sight and non-line of sight absolute range errors with true range, Kio System.

Observations from the LOS and NLOS results

▪ Accuracy shows similar behavior like BeSpoon phone until 10m distance for LOS sight setup.

▪ Error in ranging is higher when there is NLOS path between the anchor and the tag.

Another experiment is conducted to assess accuracy of trilateration of the system. Evaluation software running on Win7 helps to visualize location of anchors and position of tag with time. Four anchors are placed at the corners of a 3x4 m room. Then, their positions are inputted to evaluation software as x, y, z coordinates. Figure 22 shows followed path with black line and measurement points with red dots. Height of tag and anchors are kept same and only 2D accuracies are observed.
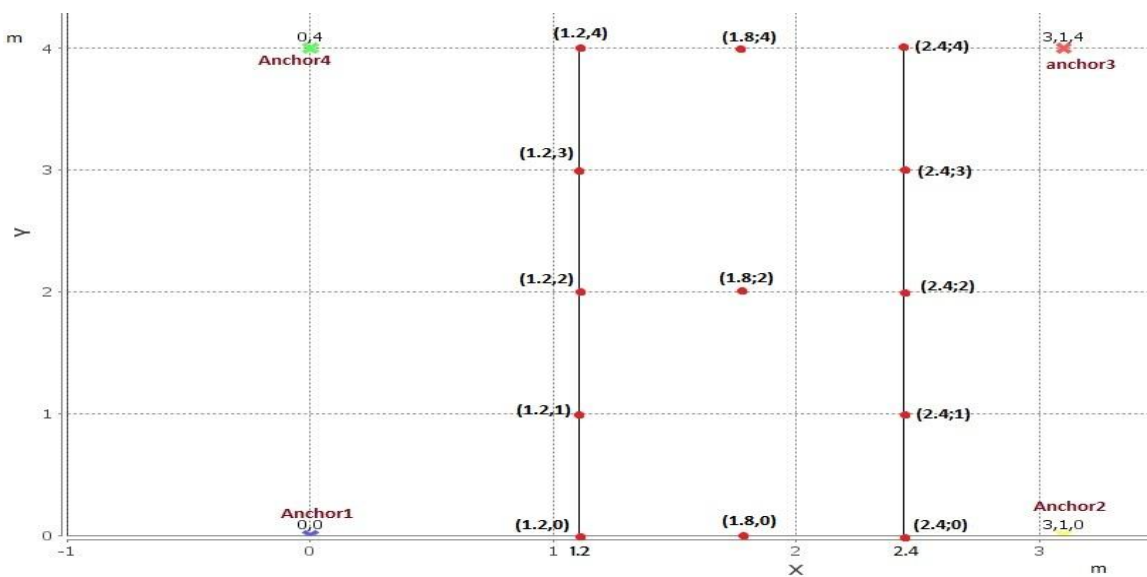
Figure 22. Measurement setup to assess accuracy of trilateration of the system.

According to the measurements, true position of each points and corresponding measurements are given in Table 10.

True position of tag (in m)	Measurement result (in m)	Absolute Errors (in cm)
(1.2; 0)	(1.04; -0.3)	(16, 30)
(1.2; 1)	(0.94; 0.73)	(26,27)
(1.2; 2)	(0.92; 1.79)	(28, 21)
(1.2; 3)	(0.81; 3.06)	(39, 6)
(1.2; 4)	(1.17; 4.4)	(3, 40)
(2.4; 0)	(2.44; -0.32)	(4, 32)
(2.4; 1)	(2.96; 0.73)	(56, 27)
(2.4; 2)	(2.87; 1.92)	(47, 8)
(2.4; 3)	(2.95; 2.91)	(55, 9)
(2.4; 4)	(2.69; 4.23)	(29, 23)
(1.8; 0)	(1.69; -0.76)	(11,76)
(1.8; 2)	(1.93; 1.92)	(13, 8)
(1.8; 4)	(1.78; 4.4)	(2, 40)

Table 10. True position of points and corresponding measurements.

From the experiment, it is observed that positioning accuracy increases when tag is close to center of the system and positioning accuracy decreases when tag is very close to one of the anchors. Positioning accuracy of 4 anchor and 1 tag is also worse than accuracy of range between one tag and one anchor.

Another experiment is conducted to obtain velocity from moving object by using similar setup as in Figure 22. Tag is moved along given trajectory during 1 minute. Trajectory of movement follows A-B, B-C, C-D, and D-A path in the Figure 23.
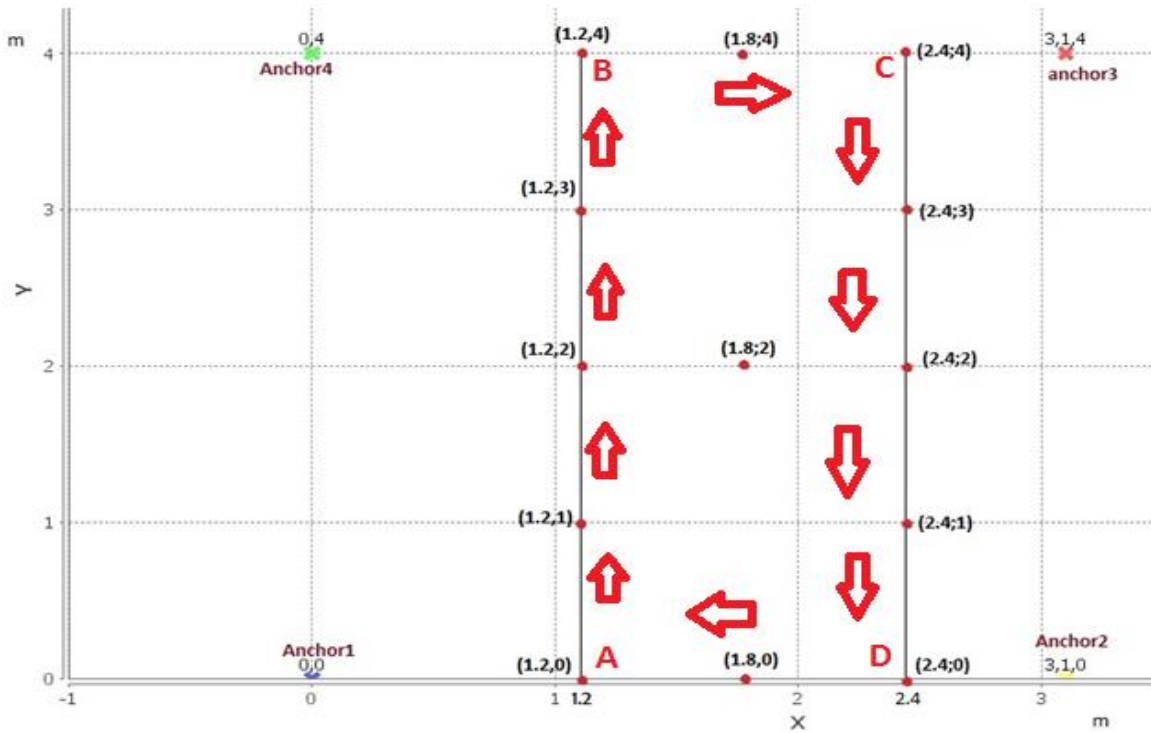
Figure 23. Measurement setup to velocity accuracy of motion.

Figure 24 shows position of tag with respect to time. Xpos with red line denotes position in x axis and Ypos with blue line denotes position in y axis.
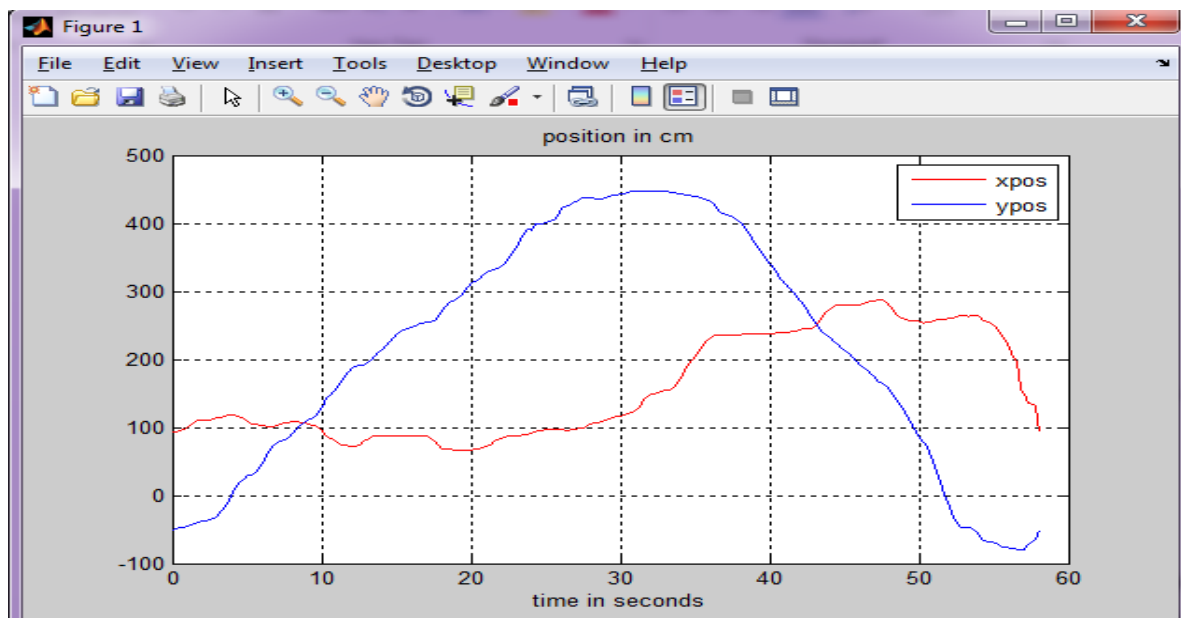
Figure 24. X and y Position of tag during motion.

The plot in Figure 24 is consistent with the motion. During first 25seconds, tag is on path A-B, between 25 and 35seconds tag is on path B-C, between 35 and 55seconds tag is on path C-D and between 55 and 60seconds tag is on path D-A.

45

From x and y positions, velocity of tag can be obtained by differentiation. Figure 25 shows velocity of tag with respect to time. Xvelocity with red line denotes velocity in x axis and Yvelocity with blue line denotes velocity in y axis.
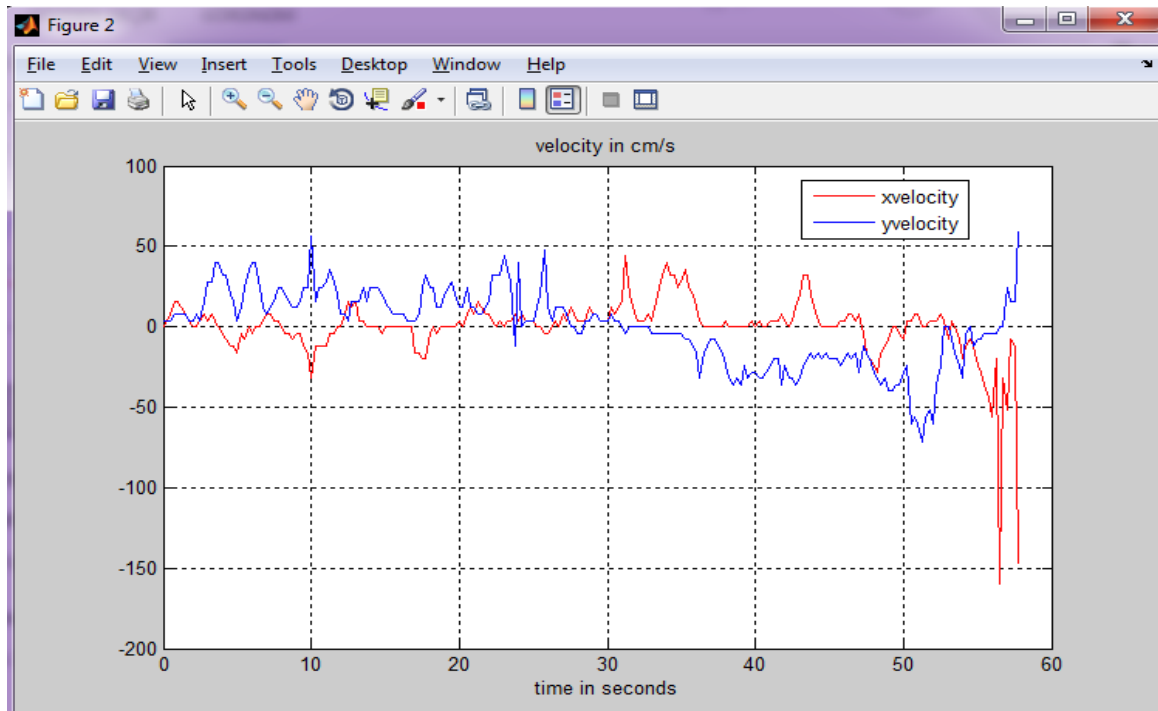
Figure 25. X and y velocity of tag during motion

Table 11 shows time intervals and mean velocities along path letters.

Path	Time interval (s)	Mean velocity (cm/s)
A-B	0-25	$V_X= 0.15$; $V_y= 18$
B-C	25-35	$V_X= 11.2$; $V_y= 3.6$
C-D	35-55	$V_x= 1.87$; $V_y= -25.2$
D-A	55-60	$V_x= -51.6$; $V_y= 7$

Table 11. x and y axis mean velocity of tag versus time interval

Similarly, velocities are consistent with the motion. Error in velocities can be observed from non-zero V_x velocities along A-B and C-D path and non-zero V_y velocities along B-C and D-A path since there is no motion in x axis along A-B and C-D path and no motion in y axis along B-C and D-A path.

46

3.2.4 FUSION OF IMU AND UWB DATA

Sensor fusion allows extracting all available information coming from sensors and combining it to obtain good estimate of desired parameters. As it is seen from stationary IMU in chapter and section 2.3.4, IMU performance in terms of velocity decreases with time due to sensor drifts. On the other hand, velocity errors do not accumulate and long term positioning with bounded errors can be obtained once the UWB setup is established. Drawbacks of UWB setup is that it slightly suffers from multi path and NLOS conditions (outliers) as observed in chapter and section 3.2.3. In order to eliminate drawbacks of each system and obtain motion tracking solution for indoor environments, robust UWB-INS sensor integration should be used. By this way, when range information is made available by UWB setup, it can fix drifted output of IMU. When there are outliers for UWB data, IMU measurements can still tide over and gives smooth solution.

Offered solution for integration IMU and UWB is similar to integration of IMU and GNSS and chapter and section 3.1.1 is devoted for algorithm of IMU and GNSS integration. While high precision GNSS systems can provide accurate velocities in north and south direction, most of the UWB systems can only provide ranges between a tag and an anchors as in the case of a Bespoon phone. In order to use the offered integration algorithm, trilaterated position of the 1tag with the presence of multiple anchors should be known to obtain velocities as in the case of Kio.

In reference [30], UWB system which consist of receivers at known positions and transmitter integrated on moving object are used with MEMS inertial measurement unit for motion tracking in indoor environments. Data from both sources is synchronized and inertial data is updated with position data coming from UWB system. Dynamic accuracies with 20 cm rms are achieved when UWB position measurements are available.

4. SUMMARY

The goal of the thesis is to investigate modern technologies that can be used in motion tracking applications and to seek alternative for complex and costly optical motion tracking systems. Inertial navigation system, high precision GNSS and ultrawide band radio beacon technologies were analyzed and selected off-the-shelf products of each technology were tested.

Xsens MTw inertial measurements unit has high update rate of up to 120Hz and it provides several parameters which could be used for human motion analysis. The parameters are 3D accelerations, velocity increments, and angular rates and coordinate transformation elements. Among these parameters, horizontal plane velocities are important in the view of human movement tracking. Moreover, Xsens unit is wearable and has wireless connectivity which makes it especially good candidate for motion tracking applications. However, as it is observed in author's experiments, Xsens sensors errors may cause considerable error in velocity calculations. Misalignment correction was implemented in MATLAB for stationary IMU as post processing of the data and it gave significant improvement in reducing velocity errors.

However, to achieve high accuracy for long duration movement tracking with IMUs, additional absolute location tracking is required. For such data logging purposes, high precision Ublox GNSS receiver was integrated with IMU device. The receiver can provide horizontal plane (north, east) velocities with accuracies of tens of centimeter per seconds. In order to track the motion, velocity data from high precision GNSS can be used to update IMU velocity information. Similar misalignment correction as in the case of stationary IMU was implemented in MATLAB to have stable and reliable velocity output. As a future work, walking and running tests should be conducted to see the improvement.

Although GNSS systems can work for outdoors with a good performance, in order to track motions in indoor environments, alternative technology is necessary. Ultrawide band radio based ToF measurement promises a good solution for indoor positioning and tracking application since due to wide pulse signal spectrum, a centimeter level measurement resolution can be achieved. Moreover, off-the-shelf UWB RTLS products are easy to be

set up and use. Author's experiments with Bespoon (France) and Kio (Estonia) systems showed that ranging accuracies are within 40cm for both system and velocity accuracy of Kio UWB is on the order on tens of centimeters per seconds. However, UWB systems are not yet integrated into author's motion tracking applications. As a future work, walking and running tests in indoors should be conducted after the integration of UWB devices with the rest of motion tracking system.

References

[1]   R. Daniel, ''Inertial and magnetic sensing of human motion'', 2006

[2]   S. Ivo, S. Tamara, P.Ante, ''Design, development and evaluation of optical motion-tracking system based on active white light markers'', IET Science, Measurement and Technology, 2013

[3]   R. Mautz, ''Indoor Positioning Technologies'', Institute of Geodesy and Photogrammetry, Department of Civil, Environmental and Geomatic Engineering, ETH Zurich, 2012

[4]   G. Alison, A. Michael, S. Joan, ''Accuracy of Inertial Motion Sensors in Static, Quasistatic, and Complex Dynamic Motion'', Journal of Biomechanical Engineering, 2009

[5]   B. Paolo, ''Wearable sensor and systems enabling technology in clinical applications'', IEEE Engineering in medicine and Biology Magazine, 2010

[6]   B. Paolo, ''Advances in wearable technology and applications in physical medicine and rehabilitation, Journal of NeuroEngineering and Rehabilitation, 2005

[7] S.P.Kwakkel, G. Lachapelle, M.E Cannon, ''GNSS Aided *In Situ* Human Lower Limb Kinematics During Running'', ION GNSS 2008, Session E3,GA, 2008

[8] P.Davidson, J. Takala, ''Algorithm for Pedestrian Navigation Combining IMU Measurement and Gait Models'', Gyroscopy and Navigation, 2013

[9] Titterton, David H., Weston, John L., ''Strapdown Inertial Navigation Technology'', Institution of Engineering and Technology, 2004

[10] W. Daehee, A. Jongsun, S. Sangkyung, H.Moonbeom, I.Sung-Hyuck, L. Young Jae, ''Performance Improvement of Inertial Navigation System by Using Magnetometer with Vehicle Dynamic Constraints'', Hindawi Publishing Corporation Journal of Sensors, 2015

[11] W. Oliver, ''An introduction to inertial navigation Oliver J. Woodman'', University of Cambridge Computer Laboratory, 2007

[12] A. Ali, N. El-Sheimy, ''Low-Cost MEMS-Based Pedestrian Navigation Technique for GPS-Denied Areas'', Journal of sensors, 2013

[13] Justin Michael B., ''Analyzing and modeling low-cost mems imus for use ın an inertial navigation system'', Worcester Polytechnic Institute, 2014

[14] Joona P., ''Strapdown inertial navigation system aiding with nonholonomic constraints using indirect Kalman filtering'', Tampere University of Technology, 2009

[15] B. Giovanni, D. Fred, S. Per, ''Xsens MTw: Miniature Wireless Inertial Motion Tracker for Highly Accurate 3D Kinematic loApplications'', Xsens Technologies, 2013

[16] G. Mohinder, W. Lawrence, A. Angus, '' Global Positioning Systems, Inertial Navigation, and Integration'', A John Wiley & Sons, Inc., Publication, 2007

[17] MTw User Manual, Xsens Technologies Document MW0502P, 2014

[18] K N Suryanarayana Rao, ''GAGAN-The indian based augmentation system'', Indian Journal of Radio & Space Physics Vol. 36, August 2007

[19] M. Pratap, E. Per, ''Global Positioning System. Signals, Measurements, and Performance'', Ganga-Jamuna Press, 2001

[20] B.Juan, W. Todd, E. Per, ''Satellite Navigation for Aviation in 2025'', 2012

[21] Ublox 7 GNSS Modules Datasheet, UBX-13003830, 2014

[22] O.Ian, H. Matti, L. Jari, ''UWB: Theory and applications'', Wiley, 2004

[23] Z. Shaghayegh, K. Bong-Soo,''UWB-Aided Inertial Motion Capture for Lower Body 3-D Dynamic Activity and Trajectory Tracking'', IEEE Transactions on Instrumentation and Measurement, 2015

[24] Z. Sahinoglu, S. Gezici and I. Guvenc, " Ultra-wideband positioning systems: theoretical limits, ranging algorithms, and protocols", Cambridge University Press, 2008

[25] Y. Mohammadreza and N.Bradford, ''Ultra Wideband Wireless Positioning Systems'', Faculty of Computer Science University of New Brunswick Fredericton, 2014

[26] C.Hasari, S.Mustafa, A.Hüseyin ''Ultrawideband Design Challenges for Wireless Chip-to-Chip Communications and Interconnects'', Aerospace Conference IEEE, 2006

[27] F.João, F.Simone, ''Mobile Positioning and Tracking: From Conventional to Cooperative Techniques''. Chichester, West Sussex, U.K.: Wiley, 2010

[28] L.Steven, Z.David, P. Kristofer, ''Radio Frequency Time-of-Flight Distance Measurement for Low-Cost Wireless Sensor Localization'', IEEE Sensor journal vol.11, No.3, 2011

[29] K. Muhammad Waqas Ahmad ''statistical sensor fusion of ultra wide band ranging and real time kinematıc satellite navigation''

[30] T. Makoto, H. Jeroen, D. Fred, L. Henk, S. Per, '' Augmentation of low cost GPS/MEMS INS with UWB positioning system for seamless outdoor/indoor positioning''

Appendix 1

```matlab
clear all;
clc;

format = '%f';
sampling_freq=120;
g= 9.8;
update_time=5;
update= update_time*sampling_freq; %number of data points during each
interval

f = importdata('MT_00210511-17h00-000.txt'); %output file from IMU

%data read from IMU
B = zeros(max(size(f))-5,18);

for i = 5:max(size(f))-1
fileID = fopen('MT_00210511-17h00-000.txt');
C = textscan(fileID, format, Inf, 'Headerlines', i, 'Delimiter', ';');
fclose(fileID);
B(i-4,:) = cell2mat(C)';
end

sizeofB=size(B,1);
measurement_time= (B(sizeofB,1)-B(1,1))/sampling_freq;

t=[0:1/sampling_freq:measurement_time];

n= round(measurement_time/update_time); %number of updates

pitch= transpose(deg2rad(B(:,17))); %pitch angle in radians
yaw= transpose(deg2rad(B(:,18)));  %yaw angle in radians
roll= transpose(deg2rad(B(:,16))); %roll angle in radians

acc_body= transpose([B(:,3) B(:,4) B(:,5)]); %body accelerations

% calculation of direct cosine matrix from euler angles

for k=1:sizeofB

Rx(:,:,k) = [ cos(roll(1,k)), 0, sin(roll(1,k)); 0, 1, 0; -
sin(roll(1,k)), 0, cos(roll(1,k))];

Ry(:,:,k) = [1 0 0; 0 cos(pitch(1,k)) -sin(pitch(1,k)); 0 sin(pitch(1,k))
cos(pitch(1,k))];

Rz(:,:,k) = [cos(yaw(1,k)) -sin(yaw(1,k)) 0; sin(yaw(1,k)) cos(yaw(1,k))
0; 0 0 1];

end
```

```matlab
for k=1:sizeofB
dcm1(:,:,k)=  ( Rx(:,:,k)*Ry(:,:,k)*Rz(:,:,k)) ;
end

%calculation of global axis accelerations from body accelerations
for k=1:sizeofB
         acc_global(:,k)= dcm1(:,:,k)*acc_body(:,k); %
end

%calculation of global axis velocities from global axis accelerations

Vx_global=cumtrapz(t,acc_global(1,:));
Vy_global=cumtrapz(t,acc_global(2,:));

% calculation of misalignment angles from velocity

delta_roll(1,1)= -(Vx_global(1,update)-Vx_global(1,1))/ (update_time*g) ;

delta_pitch(1,1)= (Vy_global(1,update)-Vy_global(1,1))/ (update_time*g) ;

delta_yaw=0;

% delta direct cosine matrix calculation from misalignment angles

delta_Rx(:,:,1) = [ cos(delta_roll(1,1)), 0, sin(delta_roll(1,1)); 0, 1,
0; -sin(delta_roll(1,1)), 0, cos(delta_roll(1,1))];

delta_Ry(:,:,1) = [1 0 0; 0 cos(delta_pitch(1,1)) -sin(delta_pitch(1,1));
0 sin(delta_pitch(1,1)) cos(delta_pitch(1,1))];

delta_Rz = [cos(delta_yaw) -sin(delta_yaw) 0; sin(delta_yaw)
cos(delta_yaw) 0; 0 0 1];

delta_dcm(:,:,1)=  delta_Rx(:,:,1)*delta_Ry(:,:,1)*delta_Rz(:,:,1);

% direct cosine matrix correction

for k=1:update
dcm_corr(:,:,k)= dcm1(:,:,k)*delta_dcm(:,:,1);
end

%corrected global axis accelerations
for k=1:update
acc_global_corr(:,k)= dcm_corr(:,:,k)*acc_body(:,k);
end

for i=2:n

delta_roll(1,i)= -(Vx_global(1,i*update)-Vx_global(1,(i-1)*update))/
(update_time*g) ;

delta_pitch(1,i)= (Vy_global(1,i*update)-Vy_global(1,(i-1)*update))/
(update_time*g) ;
```

```matlab
delta_yaw=0;


delta_Rx(:,:,i) = [ cos(delta_roll(1,i)), 0, sin(delta_roll(1,i)); 0, 1,
0; -sin(delta_roll(1,i)), 0, cos(delta_roll(1,i))];

delta_Ry(:,:,i) = [1 0 0; 0 cos(delta_pitch(1,i)) -sin(delta_pitch(1,i));
0 sin(delta_pitch(1,i)) cos(delta_pitch(1,i))];

delta_Rz(:,:,i) = [cos(delta_yaw) -sin(delta_yaw) 0; sin(delta_yaw)
cos(delta_yaw) 0; 0 0 1];

delta_dcm(:,:,i)=  delta_Rx(:,:,i)*delta_Ry(:,:,i)*delta_Rz(:,:,i);

for k=(i-1)*update:i*update
dcm_corr(:,:,k)= dcm1(:,:,k)*delta_dcm(:,:,i);
end

for k=(i-1)*update:i*update
acc_global_corr(:,k)= dcm_corr(:,:,k)*acc_body(:,k);
end

Vx_global_corr(1,1:n*update)=cumtrapz(t(1:n*update),acc_global_corr(1,1:n
*update));
Vy_global_corr(1,1:n*update)=cumtrapz(t(1:n*update),acc_global_corr(2,1:n
*update));
```